Light propagation in periodically modulated complex waveguides

Sean Nixon and Jianke Yang*
Department of Mathematics and Statistics, University of Vermont, Burlington, Vermont 05401, USA
(Received 15 December 2014; published 5 March 2015)

Light propagation in optical waveguides with periodically modulated index of refraction and alternating gain and loss are investigated for linear and nonlinear systems. Based on a multiscale perturbation analysis, it is shown that for many non-parity-time- ($\mathcal{PT}$-) symmetric waveguides, their linear spectrum is partially complex; thus light exponentially grows or decays upon propagation, and this growth or decay is not altered by nonlinearity. However, several classes of non-$\mathcal{PT}$-symmetric waveguides are also identified to possess all-real linear spectrum. For $\mathcal{PT}$-symmetric waveguides, phase transition is predicted analytically. In the nonlinear regime longitudinally periodic and transversely quasilocalized modes are found for $\mathcal{PT}$-symmetric waveguides both above and below phase transition. These nonlinear modes are stable under evolution and can develop from initially weak initial conditions.

DOI: 10.1103/PhysRevA.91.033807 PACS number(s): 42.65.Tg, 05.45.Yv

I. INTRODUCTION

Parity-time- ($\mathcal{PT}$-) symmetric wave systems have the unintuitive property that their linear spectrum can be completely real even though they contain gain and loss [1]. In spatial optics, $\mathcal{PT}$-symmetric systems can be realized by employing symmetric index guiding and an antisymmetric gain-loss profile [2–4]. In temporal optics and other physical settings, $\mathcal{PT}$-symmetric systems can be obtained as well [5–12]. So far, a number of novel phenomena in optical $\mathcal{PT}$ systems have been reported, including phase transition, nonreciprocal Bloch oscillation, unidirectional propagation, distinct pattern of diffraction, formation of solitons and breathers, wave blowup, and so on [1–6,9,13–23]. Novel photonic devices such as $\mathcal{PT}$ lasers have also been demonstrated [12].

Research into optical $\mathcal{PT}$ systems has been largely devoted to waveguides where the gain and loss is distributed along the transverse direction. This leads to the following natural question: what role does $\mathcal{PT}$ symmetry play when the gain and loss is distributed in the direction of propagation? In the study of $\mathcal{PT}$ systems which exhibit unidirectional propagation or Bragg solitons [9,16,17], this has been touched upon. However, the models in those works ignored the transverse effects on light propagation. For real waveguides (i.e., without gain and loss), control of light through modulation of the refractive index has been well documented [24], and just recently researchers have studied these modulations with added gain and loss distributed in the transverse direction [25].

In this article, we study the propagation of light in complex waveguides with periodically modulated index of refraction as well as alternating gain and loss along the direction of propagation. When this system is non-$\mathcal{PT}$ symmetric, we show that linear modes often grow or decay over distance, and this growth or decay is not affected by nonlinearity. However, several classes of non-$\mathcal{PT}$-symmetric waveguides are found to possess completely real linear spectrum, thus all linear modes propagate periodically over distance. For $\mathcal{PT}$-symmetric waveguides, phase transition is predicted analytically and verified numerically. In the nonlinear regime, families of longitudinally periodic and transversely quasilocalized solutions exist for $\mathcal{PT}$-symmetric waveguides both below and above phase transition. These nonlinear modes are stable under evolution and can develop from weak initial conditions. By applying multiscale perturbation theory, a reduced ordinary differential equation is derived for the modes' linear and nonlinear propagation, and this reduced model agrees well with direct simulations of the original system.

Propagation of light in a modulated waveguide with gain and loss can be modeled under paraxial approximation by the following nonlinear Schrödinger equation:

$$i\psi_z + \psi_{xx} + V(x,z)\psi + \sigma|\psi|^2\psi = 0, \tag{1}$$

where z is the direction of propagation, x is the transverse direction, ψ is the envelope function of the light's electric field, $V(x,z)$ is a complex periodic potential whose real part is the refractive index of the waveguide and the imaginary part represents gain and loss (negative imaginary part for gain and positive imaginary part for loss), and σ is the coefficient of the cubic nonlinearity. A schematic diagram of our system is given in Fig. 1. The paraxial model (1) is valid when the waveguide modulation is weak and the light frequency is not near the Bragg frequency of the periodic waveguide, in which case back wave reflection is negligible. This waveguide would be $\mathcal{PT}$ symmetric if

$$V^*(x,z) = V(x,-z), \tag{2}$$

where the asterisk represents complex conjugation. Note that, in this $\mathcal{PT}$ condition, coordinate reflection is only in the z direction, not x direction. This differs from the usual multidimensional $\mathcal{PT}$ symmetry [13] and more resembles the partial $\mathcal{PT}$ symmetry proposed in [26].

To be consistent with the paraxial approximation, in this article we consider complex waveguides where the z-direction modulation appears as a small perturbation,

$$V(x,z) = V_0(x) + \epsilon V_1(x,z), \tag{3}$$

where $V_0(x)$ is the unperturbed real refractive index which is assumed to be localized, $\epsilon \ll 1$, and the perturbation $V_1(z,x)$ is periodically modulated along the z direction whose period is normalized as 2π. Assuming $V_1(x,z)$ has the same transverse

*jxyang@uvm.edu

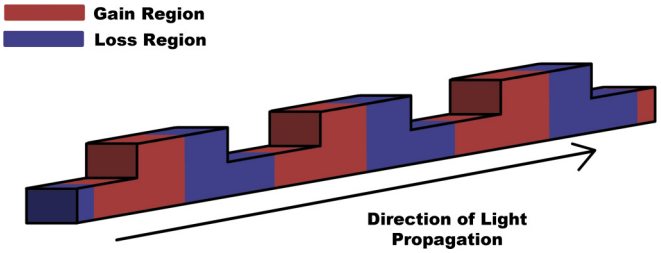

FIG. 1. (Color online) Schematic diagram for an optical waveguide with modulated index of refraction and alternating gain-loss regions. The periodic change in height represents the change in index of refraction, while the alternating regions of red and blue represent regions of gain and loss.

profile as the unperturbed index $V_0(x)$, V_1 then can be expanded into a Fourier series

$$V_1(x,z) = V_0(x)\sum_{n=-\infty}^{\infty} a_n e^{inz}, \tag{4}$$

where a_n are complex Fourier coefficients. Without loss of generality, we take $a_0 = 0$. The perturbed waveguide is $\mathcal{PT}$ symmetric when all the Fourier coefficients a_n are strictly real.

II. MULTISCALE PERTURBATION ANALYSIS

Assume that the unperturbed real waveguide V_0 supports a linear discrete eigenmode $\psi = u_0(x)e^{-i\mu_0 z}$, where μ_0 is a real propagation constant and u_0 is a real localized function satisfying

$$(\partial_{xx} + V_0 + \mu_0)u_0 = 0. \tag{5}$$

Then in the presence of the above longitudinal waveguide perturbations and weak nonlinearity, the perturbed solution to Eq. (1) can be expressed as

$$\psi(x,z) = u(x,z,Z)e^{-i\mu_0 z}, \tag{6}$$

where

$$u(x,z,Z) = \epsilon A(Z)u_0(x) + \epsilon^2 A(Z)u_1(x,z) + \epsilon^3 U_2 + \cdots, \tag{7}$$

$A(Z)$ is a slowly varying complex envelope function, and $Z = \epsilon^2 z$ is the slow distance variable. Substituting this expansion into Eq. (1), at order ϵ^2 we have

$$(i\partial_z + \partial_{xx} + V_0 + \mu_0)u_1 = -u_0 V_1.$$

Defining the operator

$$L_n = \partial_{xx} + V_0 + \mu_0 - n,$$

and expanding the solution $u_1(x,z)$ into a Fourier series

$$u_1(x,z) = \sum_{n=-\infty}^{\infty} u_1^{(n)}(x)e^{inz},$$

each term $u_1^{(n)}(x)$ is then determined from the equation

$$L_n u_1^{(n)}(x) = -a_n u_0(x)V_0(x). \tag{8}$$

Since $a_0 = 0$, the right-hand side is zero for $n = 0$. Without loss of generality we take $u_1^{(0)}(x) = 0$ as well. Since the potential $V_0(x)$ is localized, assuming no other discrete eigenvalues of V_0 differ from μ_0 by an integer, then when $n > \mu_0$ there is no solvability condition and a localized real solution $u_1^{(n)}(x)$ is admitted. When $n < \mu_0$, however, the L_n operator has nonvanishing bounded homogeneous solutions, and as a result the corresponding solution $u_1^{(n)}$ is nonvanishing at large $|x|$ as well if $a_n \neq 0$. In this case, for the solution to make sense physically, $u_1^{(n)}$ may be uniquely determined by imposing the Sommerfeld radiation condition, which says that the energy radiation must travel away from the source. In the present context, this condition translates to the boundary conditions

$$u_1^{(n)}(x) \to \begin{cases} R_+ e^{ikx}, & x \gg 1, \\ R_- e^{-ikx}, & x \ll -1, \end{cases} \tag{9}$$

where $k = \sqrt{\mu_0 - n}$ and $R_\pm$ are complex constants which measure the radiation amplitudes at $x \to \pm\infty$. A consequence of the Sommerfeld radiation condition is that the resulting physical solution $u_1^{(n)}(x)$ must be complex. To impose these boundary conditions, we write the solution $u_1^{(n)}(x)$ as

$$u_1^{(n)}(x) = \mathrm{U}_P(x) + C_1\mathrm{U}_{H1}(x) + C_2\mathrm{U}_{H2}(x),$$

where $\mathrm{U}_P(x)$ is a real particular solution to Eq. (8) and $\mathrm{U}_{H1}(x)$, $\mathrm{U}_{H2}(x)$ are two real homogenous solutions. Utilizing the boundary conditions of these homogeneous and particular real solutions and enforcing the Sommerfeld radiation condition (9), radiation amplitudes $R_\pm$ and constants $C_{1,2}$ can then be derived.

At order ϵ^3 Eq. (1) gives

$$(i\partial_z + \partial_{xx} + V_0 + \mu_0)U_2 = -iA_Z u_0 - Au_1 V_1 - \sigma|A|^2 A u_0^3.$$

Decomposing the solution U_2 into a Fourier series in z, the equation for the constant mode $U_2^{(0)}$ is found to be

$$L_0 U_2^{(0)} = -iA_Z u_0 + A\sum_{m=-\infty}^{\infty} a_{-m}a_m \tilde{u}_1^{(m)} V_0 - \sigma|A|^2 A u_0^3,$$

where $u_1^{(m)} = -a_m\tilde{u}_1^{(m)}$, and

$$L_m\tilde{u}_1^{(m)} = u_0 V_0.$$

In view of Eq. (5), u_0 is a homogeneous solution of the above inhomogeneous equation. Since L_0 is self-adjoint, in order for this equation to be solvable, its right-hand side must be orthogonal to u_0. This solvability condition leads to the following ordinary differential equation (ODE) for the evolution of the slowly varying envelope function $A(Z)$:

$$A_Z + i\tilde{\mu}A - i\tilde{\sigma}|A|^2 A = 0, \tag{10}$$

where

$$\tilde{\mu} = \sum_{m=-\infty}^{\infty} a_{-m}a_m \frac{\int_{-\infty}^{\infty} V_0 u_0 \tilde{u}_1^{(m)} dx}{\int_{-\infty}^{\infty} u_0^2 dx}, \quad \tilde{\sigma} = \sigma\frac{\int_{-\infty}^{\infty} u_0^4 dx}{\int_{-\infty}^{\infty} u_0^2 dx}. \tag{11}$$

This reduced ODE model will be helpful for the understanding of linear and nonlinear dynamics of solutions in the original equation (1) as we will elucidate below.

First we consider the solution to the linear equation (10), i.e., with the cubic term in (10) dropped. As a concrete example

we take a waveguide where all modulations of V_1 are in the first harmonics,

$$V_1(x,z) = V_0(x)(e^{iz} + \beta e^{-iz}), \tag{12}$$

where β is a complex constant. In this case, $\tilde{\mu} = \beta c$, where

$$c = \frac{\int_{-\infty}^{\infty} V_0 u_0 (\tilde{u}_1^{(-1)} + \tilde{u}_1^{(1)}) dx}{\int_{-\infty}^{\infty} u_0^2 dx}. \tag{13}$$

Recall from the earlier text that the solution $u_1^{(n)}$ is real when $n > \mu_0$ and complex when $n < \mu_0$, so is $\tilde{u}_1^{(n)}$. Thus the constant c will be real when $\mu_0 < -1$ and complex when $\mu_0 > -1$.

Since $\tilde{\mu} = \beta c$, the linear envelope equation (10) yields

$$A(Z) = A_0 e^{-i\beta c Z}, \tag{14}$$

where A_0 is the initial envelope value. In view of Eqs. (6) and (7), this $A(Z)$ solution can be absorbed into a shift of the eigenvalue

$$\mu = \mu_0 + \epsilon^2 \beta c \tag{15}$$

in the linear Bloch mode of Eq. (1),

$$\psi(x,z) = e^{-i\mu z} u(x,z). \tag{16}$$

Then we immediately see that for generic complex β values in the first-harmonic perturbation (12), a complex eigenvalue bifurcates out from every discrete real eigenvalue of the unperturbed waveguide. Even for real β values in that waveguide perturbation, a complex eigenvalue can still bifurcate out if c is complex, and this eigenvalue yields an exponentially growing eigenmode for one sign of β. Noticing this waveguide perturbation (12) is $\mathcal{PT}$ symmetric when β is real, we conclude that the linear spectrum of the waveguide is generically partially complex when the waveguide is non-$\mathcal{PT}$ symmetric. In addition, when the waveguide is $\mathcal{PT}$ symmetric, phase transition can still occur at $\beta = 0$, where exponentially growing modes appear in the linear spectrum.

Next we consider the solution to the nonlinear ODE (10). This nonlinear equation is exactly solvable, and its general solution is

$$A(Z) = A_0 \exp\left[-i\tilde{\mu} Z - i \frac{\tilde{\sigma} |A_0|^2}{2\,\mathrm{Re}[i\tilde{\mu}]} (e^{-2\,\mathrm{Re}[i\tilde{\mu}]Z} - 1)\right], \tag{17}$$

where A_0 is the initial envelope value. The amplitude of this nonlinear solution evolves as

$$|A(Z)| = |A_0| e^{-\mathrm{Re}[i\tilde{\mu}]Z}, \tag{18}$$

which is exactly the same as that of the linear solution $A(Z) = A_0 e^{-i\tilde{\mu}Z}$. This indicates that nonlinearity does not affect the magnitude of the envelope solution (regardless whether the nonlinearity is self-focusing or self-defocusing). In particular, for the first-harmonic perturbation (12) where $\tilde{\mu} = \beta c$, when $\mathrm{Re}[i\beta c] < 0$, the linear solution will grow exponentially. In this case, nonlinearity will not arrest this exponential growth at larger amplitudes.

The above predictions for the solution dynamics are verified with direct numerical computations of the original system (1). For this purpose, we first take

$$V_0 = 2\,\mathrm{sech} x, \quad \epsilon = 0.2 \tag{19}$$

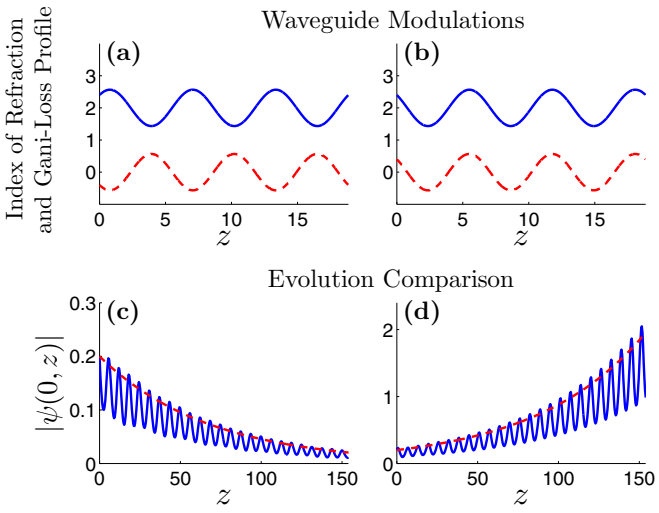

FIG. 2. (Color online) (a),(b) z-direction modulations of the waveguide (3) at $x = 0$ for $\beta = i$ and $\beta = -i$ in the first-harmonic perturbations (12) with parameters (19), respectively; solid blue is refractive-index variation and dashed red gain-loss variation (positive for gain and negative for loss); (c),(d) amplitude evolution in the nonlinear simulation of Eq. (1) with $\sigma = 1$ for $\beta = i$ and $\beta = -i$, respectively; the analytical solution is also plotted as dashed red lines for comparison.

in our waveguides (3) and (12). In this case, the unperturbed real waveguide V_0 has a single discrete eigenvalue $\mu_0 \approx -1.245 < -1$; hence c is real and numerically found to be $c \approx -0.369$. Then our theoretical analysis predicts that for any nonreal value of β in the first-harmonic perturbation (12), a complex eigenvalue bifurcates out from μ_0 according to formula (15). Numerically this is confirmed. In addition, it is found that this bifurcated eigenvalue is the only complex eigenvalue in the linear spectrum. To verify the nonlinear amplitude formula (17), we choose two β values of i and $-i$. The corresponding z-direction modulations of the perturbed waveguide at $x = 0$ are displayed in Figs. 2(a) and 2(b), respectively. In these perturbed waveguides, we take the initial condition $\psi(x,0) = \epsilon A_0 u_0(x)$, where $A_0 = 1$ and $u_0(x)$ is the eigenmode of eigenvalue μ_0 in the unperturbed waveguide V_0 with normalized peak height of 1. The simulation of the original equation (1) under this initial condition is plotted in Figs. 2(c) and 2(d) for $\beta = i$ and $-i$, respectively. Here the solution's amplitude at $x = 0$ versus z is displayed. For comparison, the analytical amplitude solution $|\epsilon A(Z) u_0(0)|$ with $|A(Z)|$ given by (18) is also plotted. As predicted by the ODE model (10), the solution for $\beta = i$ exponentially decays, while that for $\beta = -i$ exponentially grows. In the latter case, this growth is not arrested by nonlinearity [even for longer distances than those shown in panel (d)], in agreement with the analytical solution (18). It is noted that amplitude oscillations in the numerical solution are due to higher-order terms in the perturbation expansion (7), which are not accounted for in our leading-order analytical solution plotted in this figure. Physically these amplitude oscillations are due to periodic gain and loss in the waveguide.

The growth and decay of solutions in Fig. 2 for different values of β can be intuitively understood. When $\mathrm{Im}(\beta) > 0$,

modulations of the real and imaginary parts of the waveguide V have a phase difference between zero and $\pi/2$. Recalling $\mathrm{Im}(V) > 0$ corresponds to loss and $\mathrm{Im}(V) < 0$ to gain, we see that the region with strongest index of refraction, where the beam is at its strongest, corresponds to a region of loss [see Fig. 2(a)]; thus the beam decays over distance. Conversely, when $\mathrm{Im}(\beta) < 0$, modulations of the real and imaginary parts of V have a phase difference between $\pi/2$ and π. This means the region with strongest index of refraction corresponds to a region of gain [see Fig. 2(b)]; thus the beam grows over distance.

The prediction of phase transition at $\beta = 0$ in the $\mathcal{PT}$-symmetric first-harmonic perturbation (12) (with real β) is also numerically confirmed. In this case, the perturbed waveguide can be rewritten as

$$V(x,z) = V_0(x)[1 + \epsilon(1+\beta)\cos z + i\epsilon(1-\beta)\sin z], \quad (20)$$

thus $1-\beta$ controls the strength of gain and loss. In the numerics, we take

$$V_0 = \mathrm{sech}x, \quad \epsilon = 0.2. \quad (21)$$

Then the unperturbed potential V_0 has a unique discrete eigenvalue $\mu_0 \approx -0.518 > -1$, which results in a complex constant $c \approx -0.014 + 0.162i$ from formula (13). Consequently Eq. (15) predicts an exponentially growing linear mode when $\beta < 0$. Since the waveguide is $\mathcal{PT}$ symmetric, all complex eigenvalues come in conjugate pairs. For $\beta < 0$ this means a pair of complex eigenvalues bifurcate out at $\beta = 0$, which is verified numerically in Fig. 3(a). As seen in the figure, the prediction from the analytical eigenvalue formula (15) matches numerical values very well.

The asymptotic nature of the eigenvalue formula (15) for $\epsilon \ll 1$ is numerically verified as well. For this purpose, we fix $\beta = 1$ and allow ϵ to vary. The imaginary part of the numerically obtained eigenvalue μ versus ϵ is displayed in Fig. 3(b). This figure reveals a quadratic dependence on ϵ when $\epsilon \ll 1$. Comparison between the numerical values and the theoretical prediction (15) as illustrated in the figure shows good agreement.

For $\beta > 0$ in the perturbed waveguide (20) and (21), the theoretical formula (14) predicts a decaying amplitude for eigenmode $u_0(x)$. This seems to suggest a complex eigenvalue (15) for a decaying eigenmode in the linear spectrum. However, due to $\mathcal{PT}$ symmetry of the waveguide, any complex eigenvalue of a decaying eigenfunction would have to be paired with the complex conjugate of this eigenvalue for a growing eigenfunction. Since our perturbation theory does not detect growth in the physical solution, we conclude that the decay of the eigenmode $u_0(x)$ for $\beta > 0$ is due to the shedding of radiation and that the spectrum remains real. This matches, numerically, both computations of the spectrum and evolutions of the initial eigenmode $u_0(x)$.

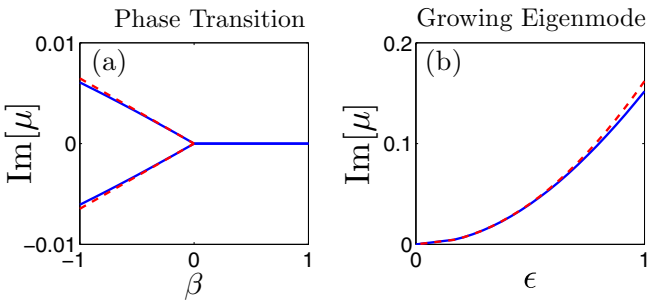

FIG. 3. (Color online) (a) Complex eigenvalues for the phase transition in β in the $\mathcal{PT}$-symmetric waveguide (20) with parameters (21). (b) Complex eigenvalue bifurcation in ϵ in the waveguide (20) with $\beta = 1$. In both figures, solid blue is numerical values and dashed red analytical predictions.

III. NON-$\mathcal{PT}$-SYMMETRIC WAVEGUIDES WITH ALL-REAL LINEAR SPECTRUM

It is seen from the previous section that, for first-harmonic perturbations (12), the linear spectrum is generically partially complex for nonreal values of β, i.e., when the perturbed waveguide is non-$\mathcal{PT}$ symmetric. However, we have found two notable families of complex waveguides which are non-$\mathcal{PT}$ symmetric but still possess all-real linear spectra. This is quite surprising, since in complex waveguides with transverse gain-loss variations, all-real spectra are very rare for non-$\mathcal{PT}$-symmetric systems [27].

The first family consists of waveguides (3) and (4) with unidirectional Fourier series decomposition, i.e., $a_n = 0$ for either $n < 0$ or $n > 0$. In our calculation of the shifted eigenvalue $\mu = \mu_0 + \epsilon^2\tilde{\mu}$ with $\tilde{\mu}$ given in Eq. (11), notice that $\tilde{\mu} = 0$ for a unidirectional Fourier series; hence the eigenvalue μ_0 does not shift at all under these complex waveguide perturbations. Regarding other eigenvalues in the linear spectrum, we have verified numerically that they do not shift to the complex plane either; thus the linear spectrum is all real for waveguides of this type.

The second family consists of separable waveguides, $V(x,z) = V_a(z) + V_b(x)$, where $\int_0^{2\pi} \mathrm{Im}[V_a(z)]dz = 0$ (meaning that the gain and loss are balanced along the propagation direction), and $V_b(x)$ is real. In this case, Bloch modes (16) in the linear equation (1) can be decomposed as $\mu = \mu_a + \mu_b$ and $u(x,z) = u_a(z)u_b(x)$, where $(u_a,\mu_a),(u_b,\mu_b)$ satisfy the following one-dimensional eigenvalue problems:

$$[i\partial_z + V_a(z)]u_a = -\mu_a u_a,$$
$$[\partial_{xx} + V_b(x)]u_b = -\mu_b u_b.$$

The first eigenvalue problem has an exact solution

$$u_a(z) = \exp\left\{i\mu_a z + i\int_0^z V_a(\xi)d\xi\right\}.$$

Thus for waveguides with equal amounts of gain and loss, i.e., $\int_0^{2\pi} \mathrm{Im}[V_a(z)]dz = 0$, its μ_a spectrum is all real. The second eigenvalue problem is a Schrödinger eigenvalue problem. Thus for real waveguides $V_b(x)$, its spectrum is also all real. Together, we see that for the separable waveguides of the above form, the linear spectrum is all real. Notice that these separable waveguides are non-$\mathcal{PT}$ symmetric in general; thus they constitute another large class of non-$\mathcal{PT}$-symmetric waveguides with all-real spectra.

IV. LONGITUDINALLY PERIODIC NONLINEAR MODES

In this section we consider nonlinear z-periodic modes in these modulated waveguides. Such modes are of the form

$$\psi(x,z) = e^{-i\mu z}u(x,z), \tag{22}$$

where μ is a real propagation constant, and $u(x,z)$ is 2π periodic in z. From the reduced ODE model (10) for the first-harmonic perturbation (12), we see that when the waveguide is non-$\mathcal{PT}$ symmetric (i.e., β is nonreal) the solution (17) will generically grow or decay (since $\tilde{\mu} = \beta c$ is generically complex); thus nonlinear z-periodic modes are not expected. But when the waveguide is $\mathcal{PT}$ symmetric and $\mu_0 < -1$, where $\tilde{\mu} = \beta c$ is real, the nonlinear solution to the ODE model is

$$A(Z) = A_0 \exp[-i\beta c Z + i\tilde{\sigma}|A_0|^2 Z]. \tag{23}$$

Since both βc and $\tilde{\sigma}$ are real, when this $A(Z)$ function is substituted into the perturbation series solution (6) and (7), analytical z-periodic nonlinear modes (22) with

$$\mu = \mu_0 + \epsilon^2(\beta c - \tilde{\sigma}|A_0|^2) \tag{24}$$

are then obtained. In this μ formula, the amplitude parameter A_0 is arbitrary. Thus a continuous family of nonlinear z-periodic modes parametrized by the propagation constant μ are predicted. Our perturbation analysis also reveals another important property about these z-periodic modes, i.e., they contain weak transversely nonlocal tails and are thus not fully localized. The order at which these nonlocal tails appear in the perturbation series depends on the unperturbed waveguide $V_0(x)$ as well as the waveguide perturbation $V_1(x)$. For the first-harmonic perturbation (12) with $V_0 = 2\,\mathrm{sech}x$ [as in (19)], $\mu_0 \approx -1.245$; thus nonlocal tails appear at the $O(\epsilon^3)$ term of expansion (7) in the e^{-2iz} harmonics. For perturbations with $V_0 = \mathrm{sech}x$ [as in (21)], $\mu_0 \approx -0.518$; thus nonlocal tails appear at the $O(\epsilon^2)$ term of expansion (7) in the e^{-iz} harmonics. Since these transversely nonlocal tails occur at higher orders of the perturbation series, the resulting z-periodic nonlinear mode is then quasilocalized, i.e., the height of the solution's tails at $x \to \pm\infty$ is much less than the solution's peak amplitude.

Numerically we have confirmed the existence of these z-periodic and transversely quasilocalized nonlinear modes in Eq. (1) for $\mathcal{PT}$-symmetric waveguides. In addition, we have found that these modes exist both below and above phase transition. These solutions are computed as a boundary value problem in the (x,z) space by the Newton-conjugate-gradient method [28]. To demonstrate, we take the first-harmonic perturbation (12) with

$$V_0 = 2\,\mathrm{sech}^2 x, \quad \epsilon = 0.2. \tag{25}$$

We also take $\sigma = 1$ (focusing nonlinearity). These waveguides with β values of 0.5 and -0.5 (below and above phase transition) are illustrated in Figs. 4(a) and 4(b), respectively. For $\beta = 0.5$ below phase transition, this family of nonlinear modes is displayed in Fig. 4(e). It is seen that these modes bifurcate from $\mu \approx -1.011$ where its amplitude approaches zero. The analytical bifurcation point from formula (24), with A_0 set to zero, is $\mu_{\mathrm{anal}} \approx -1.014$, since $\mu_0 = -1$ and $c \approx -0.691$ for the present waveguide. Apparently the numerical and analytical bifurcation points are in good agreement. Further comparison between the numerically obtained peak amplitudes of these modes and analytically obtained ϵA_0 values from Eq. (24) for varying μ values can be seen in Fig. 4(e). An example solution, with $\mu = -1.04$, is shown in Fig. 4(c). Notice that this solution is strongly localized, since its nonlocal transverse tails are very weak and thus almost invisible.

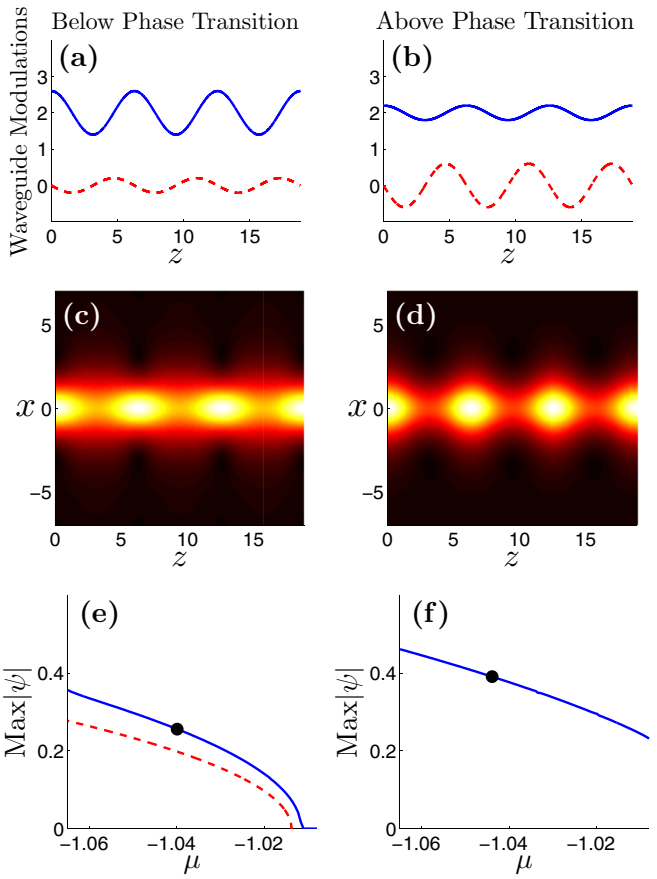

FIG. 4. (Color online) Families of longitudinally periodic and transversely quasilocalized nonlinear modes in $\mathcal{PT}$-symmetric waveguides below and above phase transition. The waveguide is (3) with first-harmonic perturbations (12) and parameters (25), and $\sigma = 1$. (a),(b) Modulated waveguides vs z at $x = 0$ for $\beta = 0.5$ (below phase transition) and $\beta = -0.5$ (above phase transition), respectively; solid blue is refractive-index variation and dashed red gain-loss variation (positive for gain and negative for loss); (c),(d) example nonlinear modes in waveguides of (a),(b), respectively; (e),(f) nonlinear modes' peak amplitude vs the propagation constant μ in waveguides of (a),(b); solid blue lines are numerical values, while the dashed red line in (e) is analytical predictions. The locations of example modes in (c),(d) are marked by black dots.

At $\beta = -0.5$ above phase transition, these nonlinear modes are found as well, whose peak amplitude versus the propagation constant μ is depicted in Fig. 4(f). These solutions do not bifurcate from infinitesimal linear modes; thus its peak amplitude does not reach zero. An example solution at $\mu = -1.044$ is shown in Fig. 4(d). This solution is also strongly localized with tails almost invisible.

We have examined the stability of these z-periodic nonlinear modes by simulating their evolution under perturbations

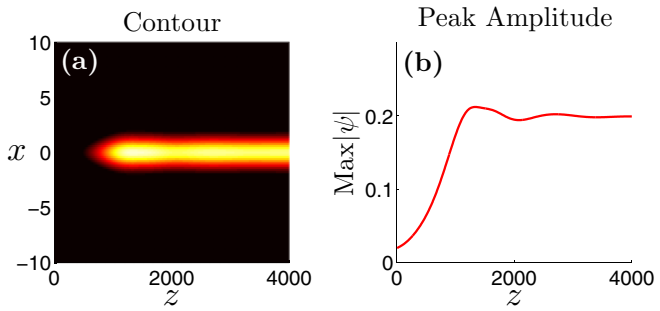

FIG. 5. (Color online) Evolution of a weak initial condition in a $\mathcal{PT}$-symmetric waveguide above phase transition. (a) Solution evolution in the (x,z) plane; (b) amplitude evolution vs distance z. In this figure, solutions are plotted at distances $z = 2n\pi$, where n is an integer; thus amplitude oscillations inside each z-period 2π (caused by gain and loss regions) are invisible.

in Eq. (1), and they are found to be stable. This stability holds even when the waveguide is above phase transition. In the latter case, an initial localized function whose amplitude is above the threshold of periodic nonlinear modes in Fig. 4(f) would evolve into one of these modes. If the initial amplitude is very small, then it will first grow exponentially due to the existence of complex (unstable) eigenvalues in the linear spectrum above phase transition. Subsequently in the nonlinear regime, we find that its growth saturates, and the solution approaches a z-periodic nonlinear state. This evolution is illustrated in Fig. 5 for the waveguide of Fig. 4(b) (with $\sigma = 1$) under the initial condition $\psi(x,0) = 0.02\,\mathrm{sech}x$. This growth saturation by nonlinearity in $\mathcal{PT}$-symmetric waveguides (above phase transition) contrasts that in non-$\mathcal{PT}$-symmetric waveguides, where the exponential growth is not arrested by nonlinearity [see Sec. II and Fig. 2(d)].

V. SUMMARY

In summary, we have studied light propagation in complex waveguides with periodic refractive-index modulations and alternating gain and loss along the direction of propagation. Our analysis is based on a multiscale perturbation theory, supplemented by direct numerical simulations. We have shown that non-$\mathcal{PT}$-symmetric waveguides often possess complex eigenvalues in their linear spectrum, but several classes of such waveguides with all-real linear spectra are also identified. We have also shown that $\mathcal{PT}$-symmetric waveguides can exhibit phase transition. In the nonlinear regime, we have shown that, for non-$\mathcal{PT}$-symmetric waveguides, cubic nonlinearity does not alter the exponential growth or decay of the related linear system. But for $\mathcal{PT}$-symmetric waveguides, continuous families of longitudinally periodic and transversely quasilocalized nonlinear modes exist both below and above phase transition. In the latter case, low-amplitude initial conditions eventually develop into these nonlinear periodic states.

ACKNOWLEDGMENTS

This work was supported in part by the Air Force Office of Scientific Research (Grant No. USAF 9550-12-1-0244) and the National Science Foundation (Grant No. DMS-1311730).

[1] C. M. Bender and S. Boettcher, Phys. Rev. Lett. **80**, 5243 (1998).
[2] R. El-Ganainy, K. G. Makris, D. N. Christodoulides, and Z. H. Musslimani, Opt. Lett. **32**, 2632 (2007).
[3] A. Guo, G. J. Salamo, D. Duchesne, R. Morandotti, M. Volatier-Ravat, V. Aimez, G. A. Siviloglou, and D. N. Christodoulides, Phys. Rev. Lett. **103**, 093902 (2009).
[4] C. E. Rueter, K. G. Makris, R. El-Ganainy, D. N. Christodoulides, M. Segev, and D. Kip, Nat. Phys. **6**, 192 (2010).
[5] A. Regensburger, C. Bersch, M. A. Miri, G. Onishchukov, D. N. Christodoulides, and U. Peschel, Nature (London) **488**, 167 (2012).
[6] R. Driben and B. A. Malomed, Opt. Lett. **36**, 4323 (2011).
[7] J. Schindler, A. Li, M. C. Zheng, F. M. Ellis, and T. Kottos, Phys. Rev. A **84**, 040101(R) (2011).
[8] H. Cartarius and G. Wunner, Phys. Rev. A **86**, 013612 (2012).
[9] L. Feng, Y. L. Xu, W. S. Fegadolli, M. H. Lu, J. E. B. Oliveira, V. R. Almeida, Y. F. Chen, and A. Scherer, Nat. Mater. **12**, 108 (2013).
[10] C. M. Bender, B. Berntson, D. Parker, and E. Samuel, Am. J. Phys. **81**, 173 (2013).
[11] B. Peng, S. Özdemir, F. Lei, F. Monifi, M. Gianfreda, G. Long, S. Fan, F. Nori, C. M. Bender, and L. Yang, Nat. Phys. **10**, 394 (2014).
[12] H. Hodaei, M.-A. Miri, M. Heinrich, D. N. Christodoulides, and M. Khajavikhan, Science **346**, 975 (2014).
[13] Z. H. Musslimani, K. G. Makris, R. El-Ganainy, and D. N. Christodoulides, Phys. Rev. Lett. **100**, 030402 (2008).
[14] S. Longhi, Phys. Rev. Lett. **103**, 123601 (2009).
[15] K. G. Makris, R. El-Ganainy, D. N. Christodoulides, and Z. H. Musslimani, Phys. Rev. A **81**, 063807 (2010).
[16] Z. Lin, H. Ramezani, T. Eichelkraut, T. Kottos, H. Cao, and D. N. Christodoulides, Phys. Rev. Lett. **106**, 213901 (2011).
[17] M. A. Miri, A. B. Aceves, T. Kottos, V. Kovanis, and D. N. Christodoulides, Phys. Rev. A **86**, 033801 (2012).
[18] F. K. Abdullaev, Y. V. Kartashov, V. V. Konotop, and D. A. Zezyulin, Phys. Rev. A **83**, 041805 (2011).
[19] S. Nixon, L. Ge, and J. Yang, Phys. Rev. A **85**, 023822 (2012).
[20] I. V. Barashenkov, S. V. Suchkov, A. A. Sukhorukov, S. V. Dmitriev, and Y. S. Kivshar, Phys. Rev. A **86**, 053809 (2012).
[21] D. A. Zezyulin and V. V. Konotop, Phys. Rev. Lett. **108**, 213906 (2012).
[22] S. Nixon, Y. Zhu, and J. Yang, Opt. Lett. **37**, 4874 (2012).
[23] Y. Lumer, Y. Plotnik, M. C. Rechtsman, and M. Segev, Phys. Rev. Lett. **111**, 263901 (2013).
[24] I. L. Garanovich, S. Longhi, A. A. Sukhorukov, and Y. S. Kivshar, Phys. Rep. **518**, 1 (2012).
[25] X. Luo, J. Huang, H. Zhong, X. Qin, Q. Xie, Y. S. Kivshar, and C. Lee, Phys. Rev. Lett. **110**, 243902 (2013).
[26] J. Yang, Opt. Lett. **39**, 1133 (2014).
[27] M. A. Miri, M. Heinrich, and D. N. Christodoulides, Phys. Rev. A **87**, 043819 (2013).
[28] J. Yang, J. Comput. Phys. **228**, 7007 (2009).